



A Left Ventricle Remodeling in Patients with Bicuspid Aortic Valve

メタデータ	言語: English 出版者: Springer Nature 公開日: 2023-12-25 キーワード (Ja): キーワード (En): Cardiac magnetic resonance, Bicuspid aortic valve, T1-mapping, Extracellular volume fraction, Electrocardiography, Transthoracic echocardiography 作成者: Suwa, Kenichiro, Rahsepar, Ali Amir, Geiger, Julia, Dolan, Ryan, Ghasemiesfe, Ahmadreza, Barker, J. Alex, Collins, D. Jeremy, Markl, Michael, Carr, C. James メールアドレス: 所属:
URL	http://hdl.handle.net/10271/0002000062

A Left Ventricle Remodeling in Patients with Bicuspid Aortic Valve

Kenichiro Suwa^{1,2*}, Amir Ali Rahsepar^{1*}, Julia Geiger^{1,3,4}, Ryan Dolan¹, Ahmadreza Ghasemiesfe^{1,5}, Alex J. Barker^{1,6}, Jeremy D. Collins^{1,7}, Michael Markl^{1,8}, James C. Carr¹

*These authors contributed equally to this work.

This study was done at Department of Radiology, Northwestern University Feinberg School of Medicine

¹Department of Radiology, Northwestern University Feinberg School of Medicine, Chicago, IL, USA,

²Division of Cardiology, Internal Medicine 3, Hamamatsu University School of Medicine, Hamamatsu, Japan

³Department of Diagnostic Imaging, University Children`s Hospital Zürich, Zürich, Switzerland

⁴University of Zürich, Zürich, Switzerland

⁵Department of Radiology, University of California Davis Medical Center, Sacramento, CA, USA

⁶Department of Radiology, University of Colorado Anschutz Medical Campus, Aurora, CO, USA

⁷Department of Radiology, Mayo Clinic, Rochester, MN, USA

⁸Department of Biomedical Engineering, Northwestern University McCormick School of Engineering, Chicago, IL, USA.

Correspondence: Kenichiro Suwa, MD. Department of Radiology, Northwestern University Feinberg School of Medicine, 737 N. Michigan Ave. Suite 1600 Chicago IL 60611, USA

Fax: +1 (312) 926-5991, Tel: +1 (312) 926-2270,

E-mail address: wapswing@gmail.com, k-suwa@hama-med.ac.jp

Acknowledgments

Funding

This work was supported by KAMIKAWA Foundation, JSPS KAKENHI (Grant number 20277353) and the National Institutes of Health (contract Grant numbers R01 HL115828 and K25 HL119608).

Abstract

Purpose: We assessed the impact of bicuspid aortic valve (BAV), aortic stenosis (AS), and regurgitation (AR) on the metrics of left ventricular (LV) remodeling, as measured by electrocardiogram (ECG), transthoracic echocardiography (TTE), and cardiac magnetic resonance (CMR).

Methods: This retrospective CMR study included 11 patients with both AS and AR (BAV-ASR), 30 with AS (BAV-AS), 28 with AR (BAV-AR), 47 with neither AS nor AR (BAV-no_AS/AR), and 40 with trileaflet aortic valve (TAV-no_AS/AR). CMR analysis included the LV end-diastolic volume index (LVEDVi), mass index (LVMI), and extracellular volume fraction (ECV). The Sokolow-Lyon and Cornell products by ECG and TTE-derived E/e' were measured.

Results: There were no differences in the ECG, TTE, and CMR parameters between BAV-no_AS/AR and TAV-no_AS/AR. However, the presence of aortic valve dysfunction resulted in an elevated Sokolow-Lyon product for BAV-ASR ($p = 0.017$) and BAV-AR ($p = 0.001$), as well as increased Cornell product ($p = 0.04$) and E/e' ($p < 0.001$) for BAV-AS compared with BAV-no_AS/AR. LVEDVi and LVMI were elevated in patients with BAV-ASR and BAV-AR compared with those with BAV-no_AS/AR (LVEDVi: 101 ± 29 ml/m² and 112 ± 32 ml/m² vs. 74 ± 15 ml/m², $p = 0.005$ and $p < 0.001$, LVMI: 75 ± 7 g/m² and 64 ± 14 g/m² vs. 47 ± 9 g/m², respectively; $p < 0.001$). There was no difference in ECV between the BAV and TAV-no_AS/AR subgroups.

Conclusion: Normally functioning BAV did not result in LV remodeling. However, concomitant AV dysfunction was associated with statistically significant morphological remodeling.

Keywords

Cardiac magnetic resonance; Bicuspid aortic valve; T1-mapping; Extracellular volume fraction;
Electrocardiography; Transthoracic echocardiography

Introduction

The bicuspid aortic valve (BAV) is the most common congenital cardiac defect, with an estimated prevalence of 0.5–2% in the general population [1]. Aortic stenosis (AS) and regurgitation (AR) are the most common complications of BAV [2-4]. Progressive aortic valve (AV) dysfunction and subsequent long-term increase in afterload and regurgitation, can lead to patients with BAV demonstrating a range of left ventricular (LV) remodeling patterns, including LV hypertrophy (LVH) and chamber enlargement. Due to heterogeneous factors with genetic predisposition and AV morphological characteristics, the relationship between BAV and LV remodeling is poorly understood.

The most widely used screening tools for LV remodeling are electrocardiography (ECG) and transthoracic echocardiography (TTE). The Sokolow-Lyon voltage/product [5] and Cornell voltage/product [6] are well-recognized measures of LVH. TTE uses tissue Doppler imaging to measure the early diastolic velocity of the mitral annulus (e'), which is an index of LV relaxation [7] and has been shown to decrease in patients with LVH [8]. In addition, the ratio of the early diastolic velocity of LV inflow (E) to e' (E/e'), an estimate of LV end-diastolic pressure [9], has been shown to increase in patients with LVH.

Cardiac magnetic resonance (CMR) is the gold standard for the quantification of global LV volume and is used for the evaluation of LV remodeling. Furthermore, pre- and post-contrast T1-mapping enables the calculation of gadolinium extracellular volume fraction (ECV), a novel measure of myocardial extracellular changes and LV fibrosis [10-15]. The purpose of our study was to investigate the impact of BAV on concomitant AV dysfunction (AS and AR) and its relationship with LV remodeling, as characterized by ECG, TTE, and CMR. We hypothesized that

ECV may be an indicator of increased fibrosis in patients with BAV, particularly in those with concomitant AV disease.

Materials and Methods

Study population

Between December 2015 and December 2016, 120 patients with BAV underwent standard-of-care CMR for the evaluation of AV function and thoracic aortic size, as well as pre- and post-contrast T1-mapping for the quantification of ECV (Figure 1). Four patients with impaired LV myocardium damaged by an etiology other than BAV (i.e., myocardial infarction, hypertrophic cardiomyopathy, cardiac amyloidosis, and ventricular septum defects) were excluded. The remaining 116 patients were classified into subgroups according to AV dysfunction. AS severity was evaluated by measuring the systolic peak velocity in the AV and AV areas (AVA) using two-dimensional (2D) cine-phase contrast (PC) MRI. The definitions of AS and AR in this study were defined as moderate or more, specifically, a peak velocity ≥ 3.0 m/s and AVA < 1.5 cm² for AS, and a regurgitant fraction $\geq 30\%$ for AR [2]. As a result, the BAV subgroups consisted of 11 patients with both AS and AR (BAV-ASR; 11 males, 55 ± 12 years), 30 with AS only (BAV-AS; 20 males, 61 ± 10 years), 28 with AR only (BAV-AR; 25 males, 46 ± 14 years), and 47 without AS or AR (BAV-no_AS/AR; 27 males, 48 ± 14 years). Of the 47 patients with a trileaflet aortic valve (TAV) who underwent CMR for the evaluation of AV function, 40 patients without AS or AR were selected (TAV-no_AS/AR; 32 males, 56 ± 16 years). This retrospective study was approved by the institutional review board (IRB). The patients were enrolled with an IRB-approved waiver of consent.

Twelve-lead ECG and TTE

Twelve-lead ECG and 2D conventional TTE were performed in 101 (87%) patients with BAV and 34 (85%) patients with TAV within 1 year of CMR. Twenty-two patients with bundle branch blocks were excluded from the analysis because of a significant effect on the ECG voltage.

The QRS duration, Sokolow-Lyon voltage/product, and Cornell voltage/product were evaluated as described previously [5, 6]. E-wave velocity using pulsed wave Doppler and e'-wave velocity of the septum using tissue Doppler in an apical 4-chamber view were measured by TTE using a commercially available system (Vivid E95, GE healthcare, Milwaukee, WI, and iE33, Philips, Bothell, WA).

MRI acquisition

All patients underwent CMR scans on a 1.5T (n = 127) or 3T (n = 29) system (Magnetom Avanto, Aera, or Skyra, Siemens Medical Systems, Erlangen, Germany). The CMR protocol included ECG-gated time-resolved 2D balanced steady state free precession (bSSFP) in the long and short axis planes, with full coverage of LV and 2D cine-PC MRI (velocity encoding, 140–500 cm/s) at the tip and below the AV for the quantification of peak velocities and regurgitant fraction. In addition, T1-mapping using a modified Look-Locker inversion recovery (MOLLI) technique was performed as previously described [12]. MOLLI images were acquired before and 10–25 minutes after contrast administration in the analysis plane set for the basal, mid, and apical LV. Gadobutrol (Bayer, Whippany, NJ) dose was 0.2 mmol/kg (glomerular filtration rate (GFR) \geq 60 ml/min/1.73 m², n = 136) or 0.1 mmol/kg (GFR 30–59 ml/min/1.73 m², n = 20). Imaging reconstruction included inline motion correction of the MOLLI images with different inversion times and calculation of parametric LV T1-maps. T1-mapping parameters were as follows: spatial resolution (SR), 1.4–1.7 \times 1.4–1.7 mm; slice thickness (SLT), 8 mm; echo time, 1.0–1.1 msec; repetition time, 2.7–4.1 msec; and flip angle, 35°. For the detection of the myocardial scar, late gadolinium enhancement (LGE), true fast imaging with SSFP (SR, 2.2 \times 2.2 mm; SLT, 6 mm), and Turbo-fast low-angle shot (SR, 1.5 \times 1.5 mm; SLT, 6 mm) images in short axis covering the whole LV were used.

MRI data analysis

The AV morphology was assessed using cine-bSSFP and 2D cine-PC MRI. The existence of linear LGE at the LV mid-wall (LGE-LVMW), LGE at the right ventricular insertion point (LGE-RVIP), LGE at locations other than the right ventricular insertion point or the mid-wall of the left ventricle (LGE-other), and LGE in the overall LV (LGE-overall) were visually evaluated. Cine-bSSFP images in a short-axis orientation covering the entire LV were used to calculate the global cardiac volume and function. Epi- and endo-cardiac contours were delineated manually from the base to the apex at the end-diastolic and end-systolic phases. The papillary muscles were considered part of the LV cavity. LV end-diastolic and end-systolic volume indices (LVEDVi and LVESVi), stroke volume index (LVSVi), mass index (LVMi), ejection fraction (LVEF), cardiac index (CI), and LV mass/LVEDV ratio (LVM/EDV) were calculated using CVI42 (V5.3, Circle Cardiovascular Imaging, Calgary, Canada).

Epi- and endo-cardiac contours and regions of interest in the LV blood pool were delineated in the base, mid, and apical LV for both pre- and post-contrast T1-mapping using CVI42. Pre- and post-contrast regional T1 values based on the AHA 16-segment model and blood pool T1 values were quantified, and regional ECV was computed using the patients' hematocrit values collected at the time of the CMR examination using the following equation: $ECV = (\Delta[1/T1_{myo}] / \Delta[1/T1_{blood}]) \times (1 - \text{hematocrit})$ [11]. The global ECV was calculated as the average of the regional ECVs. To detect diffuse fibrosis associated with BAV, regions with LGE-LVMW (19 patients, 56 segments) were included in the global ECV calculation, because they represent diffuse fibrosis[16], whereas regions with LGE-RVIP [17] and LGE-other were excluded.

Image analysis was performed by one physician (AAR) and repeated by another physician (KS) in 30 patients to assess inter-observer variability. Both physicians have more than 5 years of experience in CMR image post processing and were blinded to each other's results.

Statistical analysis

The Kolmogorov-Smirnov test was used to assess the assumption of a normal distribution. Continuous variables were compared using one-way analysis of variance (normal distribution) or the Kruskal-Wallis test (non-normal distribution). If these tests determined that a difference was significant, multiple comparisons for all groups were performed using the Tukey test (normal distribution) or the Scheffe test (non-normal distribution). Categorical variables were compared using the Chi-squared test or Fisher's exact test for expected sample numbers of less than 5. Correlation analyses were performed using Pearson's (r) test for normally distributed data or Spearman's (r_s) test for non-normally distributed data to test for associations between ECG, TTE, and CMR parameters. Receiver operating characteristic (ROC) analyses were performed for the prediction of AV dysfunction and subsequent LVH in patients with BAV. Inter-observer variability was evaluated using the intraclass correlation coefficient (ICC). An ICC value above 0.8 was considered excellent agreement. Statistical significance was set at $p < 0.05$. Statistical analyses were performed using SPSS (V17.0, IBM, Armonk, NY, USA).

Results

Patient characteristics

BAV-ASR comprised one patient with severe AS and severe AR, five patients with severe AS and moderate AR, one patient with moderate AS and Severe AR, and four patients with moderate AS and moderate AR. BAV-AS comprised 19 patients with severe AS and 11 patients with moderate AS. BAV-AR comprised six patients with severe AR and 21 patients with moderate AR. Twelve patients with TAV presented with mild AR. Sievers classification of BAV [18] included six patients with type 0, seventy-five patients with type 1, three patients with type 2, and two patients who could not be classified into any class. As summarized in Table 1, hypertension demonstrated a trend towards a higher incidence in TAV patients than in BAV patients. Images of the CMR, ECG, and TTE in the representative BAV subgroup are shown in Figure 2.

ECG and TTE characteristics

As summarized in Table 2, there was no difference in ECG and TTE parameters between patients with BAV-no_AS/AR and those with TAV-no_AS/AR. The Sokolow-Lyon product was significantly greater in patients with BAV-ASR and BAV-AR than in those with BAV-no_AS/AR (269 ± 80 mVms and 266 ± 129 mVms vs. 183 ± 68 mVms, $p = 0.02$ and $p = 0.001$, respectively). Cornell product was significantly higher in patients with BAV-AS than in those with BAV-no_AS/AR (197 ± 136 mVms vs. 133 ± 65 mVms, $p = 0.04$). e' was significantly decreased and E/e' was significantly increased in patients with BAV-AS compared with patients with BAV-no_AS/AR (e' : 7.01 ± 1.87 cm/s vs. 8.73 ± 2.31 cm/s, respectively, $p = 0.04$, E/e' : 14.4 ± 5.5 vs. 9.9 ± 3.8 , respectively, $p < 0.001$).

LGE, Global LV volumetric characteristics and ECV by CMR

As summarized in Table 3, the overall prevalence of LGE-overall in patients with BAV was more than half the prevalence in patients with AS (55% in BAV-ASR, 50% in BAV-AS) but less than 20% in patients without AS (21% in BAV-AR, 17% in BAV-no_AS/AR) ($p = 0.008$). There were no differences between the subgroups in terms of LGE-RVIP ($p = 0.22$) and LGE-LVMW ($p = 0.40$). However, there was a significant difference ($p = 0.001$) in LGE-others between the subgroups.

There were no differences in global LV volume, function parameters, and ECV between patients with BAV-no_AS/AR and those with TAV-no_AS/AR. However, LVEDVi, LVSVi, and LVMi were significantly higher in patients with BAV-ASR and BAV-AR than in those with BAV-no_AS/AR (LVEDVi: 101 ± 29 ml/m² and 112 ± 32 ml/m² vs. 74 ± 15 ml/m², $p = 0.005$ and $p < 0.001$, LVSVi: 60 ± 13 ml/m² and 66 ± 17 ml/m² vs. 46 ± 10 ml/m², $p = 0.003$ and $p < 0.001$, LVMi: 75 ± 7 g/m² and 64 ± 14 g/m² vs. 47 ± 9 g/m², respectively, $p < 0.001$). In patients with BAV-AS, LVMi and LVM/EDV exhibited a significant increase compared with patients with BAV-no_AS/AR (LVMi; 57 ± 15 g/m² vs. 47 ± 9 g/m², $p = 0.003$, LVM/EDV; 0.82 ± 0.26 g/ml vs. 0.66 ± 0.18 g/ml, $p = 0.004$). ECV demonstrated no differences between the BAV subgroups.

Inter-observer variabilities were excellent for LVEDVi (ICC, 0.99; 95% confidence interval (CI), 0.99-1.00), LVESVi (ICC, 1.00; 95% CI, 0.99-1.00), SVi (ICC, 0.99; 95% CI, 0.98-1.00), EF (ICC, 0.99; 95% CI, 0.97-0.99), C.I. (ICC, 0.99; 95% CI, 0.97-1.00), LVMi (ICC, 0.98; 95% CI, 0.95-0.99) and ECV (ICC, 0.98; 95% CI, 0.95–0.99).

Correlation between ECG, TTE, and CMR parameters

As summarized in Figure 3a, 3b, 3e, and 3f, moderate positive correlations were found between the global LV function parameters (LVEDVi and LVMi) and Sokolow-Lyon parameters (Sokolow-Lyon voltage and product) ($r_s = 0.47$ – 0.50 ; $p < 0.001$). Mild or moderate positive

correlations were detected between the LV function parameters (LVEDVi and LVMi) and Cornell parameters (Cornell voltage and product) ($r_s = 0.19-0.40$; $p = 0.001-0.047$) (Figure 3c, 3d, 3g, and 3h). e' showed a mild positive correlation with LVSVi ($r_s = 0.35$, $p < 0.001$, Figure 4a) and a mild negative correlation with LVM/EDV ($r_s = -0.36$, $p < 0.001$, Figure 4b). Finally, ECV and LVMi showed moderate negative correlations with BAV-no_AS/AR ($r_s = -0.38$, $p = 0.009$) and TAV-no_AS/AR ($r_s = -0.43$, $p = 0.009$) (Figure 5).

ROC analysis for the prediction of AV dysfunction and LVH

For the prediction of severe AS by LVMi, ROC analysis showed an area under the curve (AUC) of 0.696 ($p = 0.006$) (Figure 6a). The sensitivity and specificity were 0.80 and 0.56, respectively, with a cutoff of ≥ 53 g/m². ROC analysis for the detection of severe AR by LVMi showed an AUC of 0.861 ($p = 0.015$) (Figure 6b). The sensitivity and specificity were 1.0 and 0.69, respectively, with a cutoff of ≥ 59.6 g/m². Using these cutoff values for LVMi, we diagnosed LVH for severe AS (AS_LVH) and severe AR (AR_LVH). For the prediction of AS_LVH, the AUC was 0.737 ($p < 0.0001$) by Sokolow-Lyon product (Figure 6c) and 0.687 ($p < 0.0001$) by Cornell product (Figure 6d). For the prediction of AR_LVH, the AUC was 0.754 ($p < 0.0001$) by Sokolow-Lyon product (Figure 6e) and 0.690 ($p < 0.001$) by Cornell product (Figure 6f). The cutoff values, sensitivity, and specificity are summarized in Table 4.

Discussion

In this study, we found that patients with BAV without AV dysfunction demonstrated no signs of LV remodeling. However, comparisons between subgroups in BAV, ECG, and TTE parameters could detect LV remodeling in patients with AV dysfunction. CMR revealed LV remodeling by altered volumetric parameters in patients with AV dysfunction, but no difference in ECV between BAV subgroups.

Our findings suggest that LV remodeling in BAV may not occur without AV dysfunction. Global volumetric remodeling, such as LV hypertrophy and/or dilatation, may develop after the prominent initiation of AS and/or AR, and can be detected using ECG metrics. LGE-overall was the highest in patients with AS. Nevertheless, there was no difference in ECV between the subgroups in terms of AV dysfunction. This difference may be secondary to separate techniques: ECV was calculated in three short-axis slices of the LV, whereas LGE was assessed in short-axis slices covering the entire LV.

LVEDVi was increased in AR, while LVM/EDV was elevated in AS in our study, supporting concentric LVH in AS and eccentric LVH in AR [19, 20]. Our comparison between BAV and TAV in patients without AS or AR revealed no differences in LVEDVi. In a previous study by Grotenhuis et al. [20], patients with non-stenotic BAV with trace or no AR demonstrated normal LVEDV, supporting our results. As reported in a previous paper [21], the global LV volume and function findings suggest that volumetric remodeling in BAV is most likely caused by concomitant AV dysfunction, rather than by BAV itself.

Konno et al. [22] reported that Sokolow-Lyon and Cornell voltage demonstrated a positive correlation with LV mass in patients with hypertrophic cardiomyopathy, and our patients with

BAV and TAV also demonstrated a positive correlation between global LV function parameters and QRS voltage parameters.

In two studies [23, 24] without a clear description of the AV type, myocardial fibrosis was established pathologically as a key process driving the progression from hypertrophy to heart failure in patients with AS and AR. In previous studies, a higher incidence of mid-wall LGE was observed in patients with AS and positively associated with LV wall thickness [13, 25] and post-operative mortality [26]. In another study of patients with AR, histological fibrosis in the LV was strongly correlated with LGE and was related to prognosis after surgery [27].

Previous studies have revealed inconsistent results regarding the relationship between AS and ECV. Studies have shown elevated ECV in AS compared to controls [10, 14], no difference in ECV between AS and controls [15], and no difference in ECV among different degrees of AS [13]. Sparrow et al. [28] used T1-mapping to evaluate diffuse LV fibrosis in patients with AR. However, no studies have examined the relationship between ECV and AR. In our study of patients with BAV, the ECV of patients with BAV-ASR, -AS, and -AR was similar to the ECV of patients with no_AS/AR. This pattern was not observed for macroscopic scarring as determined by LGE, as patients with AS demonstrated a higher prevalence of LGE. This discordance may be due to technical differences, that is, LGE highlighted the region with the most severe fibrosis, whereas ECV quantified the average value across the entire LV. Interestingly, in a recent study by Inoue et al. [29], ECV was negatively correlated with Sokolow-Lyon and Cornell voltages in patients without marked LVH. As shown in Figure 5, ECV and LVMi showed a negative correlation in BAV-no_AS/AR and TAV-no_AS/AR, while there was a trend towards a positive correlation in BAV with AV dysfunction ($r = 0.24, p = 0.059$), resulting in no significant correlation in the overall cohort. It has been speculated that ECV in patients with AV dysfunction may be associated with

an increase in LVMi. However, etiologies other than AV disease may mask the positive correlation between LVMi and ECV in the entire BAV cohort. In summary, the assessment of LV fibrosis in BAV using ECV may not supersede LGE.

This study has several limitations. All the patients enrolled in this study had a peculiar background, in that they had symptoms that needed to be referred for CMR evaluation. Regarding this background, TAV-no_AS/AR exhibited a relatively large number of LGE images. Nevertheless, the ECV value in TAV-no_AS/AR seemed to be acceptable for normal controls. The sample size of patients with BAV-ASR was too small to show statistical significance. Demographic differences between the subgroups included a higher percentage of males in the BAV-ASR and BAV-AR subgroups, although this difference was not significant. An older age in the BAV-AS subgroup was also observed, which may be reflected by the nature of AS. The retrospective nature of the study limited the assessment of the causality between AV dysfunction and ECV elevation. This study lacked TAV subgroups with AS and AR to elucidate the differences in LV remodeling between BAV and TAV, independent of the severity of AV dysfunction. Finally, no routine assessment was performed for mitral regurgitation using TTE, which is known to affect e' and E/e' values; however, no patient with moderate or severe mitral regurgitation by CMR was included in the study.

In conclusion, this study aimed to clarify the LV remodeling that occurs in patients with BAV, as assessed by ECG, TTE, and CMR. Morphological and functional LV remodeling were associated with AV dysfunction in patients with BAV, rather than this being a consequence of BAV alone, while microscopic fibrosis by ECV was associated with neither AV dysfunction nor BAV itself. Larger prospective longitudinal cohort studies quantifying ECV, LV function, and

LGE in subgroups and the severity of AV dysfunction are warranted to further elucidate the association between BAV and LV remodeling.

References

1. Siu SC, Silversides CK (2010) Bicuspid aortic valve disease. *J Am Coll Cardiol* 55:2789–2800. <https://doi.org/10.1016/j.jacc.2009.12.068>
2. Bonow RO, Carabello BA, Chatterjee K, et al (2006) ACC/AHA 2006 guidelines for the management of patients with valvular heart disease: A report of the American College of Cardiology/American Heart Association Task Force on Practice Guidelines (writing committee to revise the 1998 guidelines for the management of patients with valvular heart disease) developed in collaboration with the Society of Cardiovascular Anesthesiologists endorsed by the Society for Cardiovascular Angiography and Interventions and the Society of Thoracic Surgeons. *J Am Coll Cardiol* 48:e1-e48.
3. Campbell M (1968) Calcific aortic stenosis and congenital bicuspid aortic valves. *Br Heart J* 30:606-616. <https://doi.org/10.1136/hrt.30.5.606>
4. Roberts WC, Morrow AG, McIntosh CL, Jones M, Epstein SE (1981) Congenitally bicuspid aortic valve causing severe, pure aortic regurgitation without superimposed infective endocarditis. Analysis of 13 patients requiring aortic valve replacement. *Am J Cardiol* 47:206-209. [https://doi.org/10.1016/0002-9149\(81\)90385-4](https://doi.org/10.1016/0002-9149(81)90385-4)
5. Sokolow M, Lyon TP (1949) The ventricular complex in left ventricular hypertrophy as obtained by unipolar precordial and limb leads. *Am Heart J* 37:161-186. [https://doi.org/10.1016/0002-8703\(49\)90562-1](https://doi.org/10.1016/0002-8703(49)90562-1)
6. Okin PM, Roman MJ, Devereux RB, Kligfield P (1995) Electrocardiographic identification of increased left ventricular mass by simple voltage-duration products. *J Am Coll Cardiol* 25:417-423. [https://doi.org/10.1016/0735-1097\(94\)00371-V](https://doi.org/10.1016/0735-1097(94)00371-V)
7. Nagueh SF, Middleton KJ, Kopelen HA, Zoghbi WA, Quiñones MA (1997) Doppler

tissue imaging: A noninvasive technique for evaluation of left ventricular relaxation and estimation of filling pressures. *J Am Coll Cardiol* 30:1527–1533.

[https://doi.org/10.1016/S0735-1097\(97\)00344-6](https://doi.org/10.1016/S0735-1097(97)00344-6)

8. Fernandes-Silva MM, Shah AM, Hegde S, et al (2017) Race-related differences in left ventricular structural and functional remodeling in response to increased afterload: The ARIC study. *JACC Heart Fail* 5:157-165. <https://doi.org/10.1016/j.jchf.2016.10.011>
9. Mottram PM, Marwick TH (2005) Assessment of diastolic function: What the general cardiologist needs to know. *Heart* 91:681-695. <https://doi.org/10.1136/hrt.2003.029413>
10. Sado DM, Flett AS, Banyersad SM, et al (2012) Cardiovascular magnetic resonance measurement of myocardial extracellular volume in health and disease. *Heart* 98:1436-1441. <https://doi.org/10.1136/heartjnl-2012-302346>
11. Kellman P, Wilson JR, Xue H, Ugander M, Arai AE (2012) Extracellular volume fraction mapping in the myocardium, part 1: Evaluation of an automated method. *J Cardiovasc Magn Reson* 14:63. <https://doi.org/10.1186/1532-429X-14-63>
12. Kellman P, Arai AE, Xue H (2013) T1 and extracellular volume mapping in the heart: Estimation of error maps and the influence of noise on precision. *J Cardiovasc Magn Reson* 15:56. <https://doi.org/10.1186/1532-429X-15-56>
13. Chin CWL, Everett RJ, Kwiecinski J, et al (2017) Myocardial fibrosis and cardiac decompensation in aortic stenosis. *JACC Cardiovasc Imaging* 10:1320-1333. <https://doi.org/10.1016/j.jcmg.2016.10.007>
14. Chin CWL, Semple S, Malley T, et al (2014) Optimization and comparison of myocardial T1 techniques at 3T in patients with aortic stenosis. *Eur Heart J Cardiovasc Imaging* 15:556-565. <https://doi.org/10.1093/ehjci/jet245>

15. Singh A, Horsfield MA, Bekele S, et al (2015) Myocardial T1 and extracellular volume fraction measurement in asymptomatic patients with aortic stenosis: Reproducibility and comparison with age-matched controls. *Eur Heart J Cardiovasc Imaging* 16:763-770. <https://doi.org/10.1093/ehjci/jev007>
16. Gulati A, Jabbour A, Ismail TF, et al (2013) Association of fibrosis with mortality and sudden cardiac death in patients with nonischemic dilated cardiomyopathy. *JAMA* 309:896-908. <https://doi.org/10.1001/jama.2013.1363>
17. Chan RH, Maron BJ, Olivotto I, et al (2015) Significance of late gadolinium enhancement at right ventricular attachment to ventricular septum in patients with hypertrophic cardiomyopathy. *Am J Cardiol* 116:436-441. <https://doi.org/10.1016/j.amjcard.2015.04.060>
18. Sievers HH, Schmidtke C (2007) A classification system for the bicuspid aortic valve from 304 surgical specimens. *J Thorac Cardiovasc Surg* 133:1226-1233. <https://doi.org/10.1016/j.jtcvs.2007.01.039>
19. Mannacio V, Guadagno E, Mannacio L, et al (2015) Comparison of left ventricular myocardial structure and function in patients with aortic stenosis and those with pure aortic regurgitation. *Cardiology* 132:111-118. <https://doi.org/10.1159/000431283>
20. Grotenhuis HB, Ottenkamp J, Westenbergh JJM, et al (2007) Reduced aortic elasticity and dilatation are associated with aortic regurgitation and left ventricular hypertrophy in nonstenotic bicuspid aortic valve patients. *J Am Coll Cardiol* 49:1660-1665. <https://doi.org/10.1016/j.jacc.2006.12.044>
21. Geiger J, Rahsepar AA, Suwa K, et al (2018) 4D flow MRI, cardiac function, and T1 - mapping: Association of valve-mediated changes in aortic hemodynamics with left

- ventricular remodeling. *J Magn Reson Imaging* 48:121-131.
<https://doi.org/10.1002/jmri.25916>
22. Konno T, Nagata Y, Teramoto R, et al (2016) Usefulness of electrocardiographic voltage to determine myocardial fibrosis in hypertrophic cardiomyopathy. *Am J Cardiol* 117:443-449. <https://doi.org/10.1016/j.amjcard.2015.11.015>
 23. Hein S, Arnon E, Kostin S, et al (2003) Progression from compensated hypertrophy to failure in the pressure-overloaded human heart: Structural deterioration and compensatory mechanisms. *Circulation* 107:984-991.
<https://doi.org/10.1161/01.CIR.0000051865.66123.B7>
 24. Elias N, Tarasoutchi F, Spina GS, et al (2009) Myocardial fibrosis and ventricular remodeling in severe chronic aortic regurgitation. *Arq Bras Cardiol* 92:63-67.
<https://doi.org/10.1590/S0066-782X2009000100010>
 25. Park J, Chang HJ, Choi JH, et al (2014) Late gadolinium enhancement in cardiac MRI in patients with severe aortic stenosis and preserved left ventricular systolic function is related to attenuated improvement of left ventricular geometry and filling pressure after aortic valve replacement. *Korean Circ J* 44:312-319.
<https://doi.org/10.4070/kcj.2014.44.5.312>
 26. Barone-Rochette G, Piérard S, De Meester De Ravenstein C, et al (2014) Prognostic significance of LGE by CMR in aortic stenosis patients undergoing valve replacement. *J Am Coll Cardiol* 64:144-154. <https://doi.org/10.1016/j.jacc.2014.02.612>
 27. Azevedo CF, Nigri M, Higuchi ML, et al (2010) Prognostic significance of myocardial fibrosis quantification by histopathology and magnetic resonance imaging in patients with severe aortic valve disease. *J Am Coll Cardiol* 56:278-287.

<https://doi.org/10.1016/j.jacc.2009.12.074>

28. Sparrow P, Messroghli DR, Reid S, et al (2006) Myocardial T1 mapping for detection of left ventricular myocardial fibrosis in chronic aortic regurgitation: Pilot study. *AJR Am J Roentgenol* 187:W630-W635. <https://doi.org/10.2214/AJR.05.1264>
29. Inoue YY, Ambale-Venkatesh B, Mewton N, et al (2017) Electrocardiographic impact of myocardial diffuse fibrosis and scar: MESA (Multi-Ethnic study of atherosclerosis). *Radiology* 282:690-698. <https://doi.org/10.1148/radiol.2016160816>

Statements and Declarations

Funding

This work was supported by KAMIKAWA Foundation, JSPS KAKENHI (Grant number 20277353) and the National Institutes of Health (contract Grant numbers R01 HL115828 and K25 HL119608).

Competing interests

The authors have no relevant financial or non-financial interests to disclose.

Author contributions

All authors contributed to the study conception and design. Material preparation, data collection and analysis were performed by Kenichiro Suwa, Amir Ali Rahsepar, and Ahmadreza Ghasemiesfe. The first draft of the manuscript was written by Kenichiro Suwa. All authors read and approved the final manuscript

Ethics approval

This retrospective study was approved by the institutional review board.

Consent to participate

The patients were enrolled with an institutional review board-approved waiver of consent.

Consent to publish

The authors affirm that human research participants provided informed consent for publication of the images in Figure 2.

Table 1. Patients' characteristics

	BAV					TAV
	ASR	AS	AR	no_AS/AR	All BAV	no_AS/AR
	(n = 11)	(n = 30)	(n = 28)	(n = 47)	(n = 116)	(n = 40)
Age, years	55 ± 12	61 ± 10* [†]	46 ± 14 [‡]	48 ± 14	51 ± 14	56 ± 16
Male, n (%)	11 (100)	20 (67)	25 (89)	27 (57)	83 (72)	32 (80)
BSA, m ²	2.02 ± 0.13	2.00 ± 0.23	2.13 ± 0.26	2.03 ± 0.24	2.04 ± 0.24	2.07 ± 0.20
Hypertension, n (%)	3 (27)	9 (30)	6 (21)	13 (28)	31 (27)	18 (45)
Smoking, n (%)	5 (46)	11 (37)	5 (18)	14 (30)	35 (30)	11(28)
Medications						
Beta blockers, n (%)	7 (64)	18 (60)	12 (43)	15 (32)	49 (42)	24 (60)
ACE-Is, n (%)	2 (18)	5 (17)	3 (11)	4 (9)	14 (12)	9 (23)
ARBs, n (%)	3 (27)	5 (17)	13 (46)	14 (30)	35 (30)	16 (40)
CCBs, n (%)	0 (0)	3 (10)	3 (11)	2 (4)	8 (7)	6 (15)
Aspirin, n (%)	5 (45)	18 (60)	10 (36)	13 (28)	46 (40)	13 (33)

ACE-Is, angiotensin converting enzyme inhibitors; ARBs, angiotensin II receptor blockers; AR, aortic regurgitation; AS, aortic stenosis; ASR, aortic stenosis and regurgitation; BAV, bicuspid aortic valve; BSA, body surface area; CCBs, calcium channel blockers; CMR, cardiac magnetic resonance; no_AS/AR, neither AS nor AR; TAV, trileaflet aortic valve. Data are presented as mean ± SD, n (%). * $p < 0.05$, compared to BAV-AR; [†] $p < 0.05$, compared to BAV-no_AS/AR; [‡] $p < 0.05$, compared to TAV-control.

Table 2. ECG and TTE characteristics between subgroups in BAV according to AS and/or AR and TAV

	BAV			TAV	
	ASR	AS	AR	no_AS/AR	no_AS/AR
	(n = 11)	(n = 30)	(n = 28)	(n = 47)	(n = 40)
ECG					
QRS, ms	105 ± 17	94±19	96±12	93±13	96±12
Sokolow-Lyon voltage, mV	2.58 ± 0.76	2.01 ± 0.73	2.75 ± 1.23*‡§	1.96 ± 0.65	1.92 ± 0.74
Sokolow-Lyon product, mVms	269 ± 80*‡§	186 ± 67	266 ± 129*‡§	183 ± 68	183 ± 70
Cornell voltage, mV	2.11 ± 0.63	2.05 ± 1.10	1.84 ± 0.65	1.51 ± 0.63	1.50 ± 0.77
Cornell product, mVms	219 ± 84	197 ± 136‡	177 ± 65	133 ± 65	141 ± 82
TTE					
e', cm/s	6.47 ± 0.79†	7.01 ± 1.87†‡	9.25 ± 2.85	8.73 ± 2.31	7.97 ± 3.09
E/e'	12.3 ± 3.8	14.4 ± 5.5†‡§	9.8 ± 3.8	9.9 ± 3.8	10.2 ± 3.7

AR, aortic regurgitation; AS, aortic stenosis; ASR, aortic stenosis and regurgitation; BAV, bicuspid aortic valve; e', early diastolic peak tissue velocity at the ventricular septum; E/e', early diastolic peak velocity of LV inflow divided by e', no_AS/AR: neither AS nor AR, TAV: trileaflet aortic valve. Data are presented as mean ± SD, n (%). *: $p < 0.05$ compared to BAV-AS, †: $p < 0.05$ compared to BAV-AR, ‡: $p < 0.05$, compared to BAV-no_AS/AR. § $p < 0.05$, compared to TAV-no_AS/AR.

Table 3. CMR characteristics compared between subgroups in BAV according to AS and/or AR and TAV

	BAV				TAV
	ASR	AS	AR	no_AS/AR	no_AS/AR
	(n = 11)	(n = 30)	(n = 28)	(n = 47)	(n = 40)
LGE-overall, n (%)	6 (55)	15 (50)	6 (21)	8 (17)	11 (28)
LGE-RVIP, n (%)	1 (10)	7 (23)	3 (11)	3 (6)	3 (8)
LGE-LVMW, n (%)	2 (18)	9 (30)	3 (11)	7 (15)	7 (18)
LGE-other, n (%)	4 (36)	2 (7)	0 (0)	1 (2)	1 (5)
LVEDVi, ml/m ²	101 ± 29*‡§	70 ± 18	112 ± 32*‡§	74 ± 15	74 ± 12
LVESVi, ml/m ²	41 ± 22*‡§	25 ± 10	45 ± 17*†‡	28 ± 8	28 ± 9
LVSVi, ml/m ²	60 ± 13*‡§	45 ± 11	66 ± 17*‡§	46 ± 10	46 ± 8
LVMi, g/m ²	75 ± 7*‡§	57 ± 15‡	64 ± 14‡§	47 ± 9	50 ± 10
LVEF, %	61 ± 12	66 ± 8	62 ± 6	62 ± 6	62 ± 8
CI, l/min/m ²	4.1 ± 0.6*‡§	2.9 ± 0.7	4.1 ± 1.1*‡§	3.0 ± 0.6	3.0 ± 0.6
LVM/EDV, g/ml	0.79 ± 0.19†	0.82 ± 0.26†‡	0.59 ± 0.15	0.66 ± 0.18	0.69 ± 0.15
ECV, %	26.2 ± 3.5	25.6 ± 2.6	25.8 ± 3.4	25.2 ± 2.6	24.6 ± 2.3

AR: aortic regurgitation, AS: aortic stenosis, ASR: aortic stenosis and regurgitation, BAV: bicuspid aortic valve, LVEF: left ventricular ejection fraction, ECV: gadolinium extracellular volume fraction, CI: cardiac index, LGE: late gadolinium enhancement, LGE-LVMW: LGE in the left ventricular mid-wall, LGE-RVIP: LGE in the RV insertion point, LGE-other: LGE other than that in RVIP and LVMW; LVEDVi: left ventricular end diastolic volume index; LVESVi: left

ventricular end systolic volume index; LVSVi: left ventricular stroke volume index; LVMi: left ventricular mass index; no_AS/AR: neither AS nor AR; TAV: trileaflet aortic valve. Data are presented as mean \pm SD, n (%). *: $p < 0.05$ compared to BAV-AS, †: $p < 0.05$ compared to BAV-AR, ‡: $p < 0.05$, compared to BAV-no_AS/AR. § $p < 0.05$, compared to TAV-no_AS/AR.

Table 4. Diagnostic accuracy for the prediction of AS_LVH and AR_LVH.

		Cutoff, mVms	Sensitivity	Specificity
AS_LVH	Sokolow-Lyon product	≥ 216.1	0.644	0.841
	Cornell product	≥ 176.2	0.544	0.770
AR_LVH	Sokolow-Lyon product	≥ 213.6	0.756	0.744
	Cornell-product	≥ 205.9	0.462	0.873

Figure legends

Fig. 1 Flow chart of patient recruitment

CMR including T1-mapping was performed in 120 patients with BAV who met the inclusion criteria. After the exclusion of four patients, 116 patients were assessed for AS and AR using CMR, and were classified into four subgroups: BAV-ASR, n=11; BAV-AS, n=30; BAV-AR, n=28; and BAV-no_AS/AR, n=47. Patients with TAV without AV dysfunction (n=40) were recruited as controls.

Fig. 2 CMR, ECG, and TTE images in representative BAV subgroups

Images are cine-bSSFP images in 4-chamber view (**a, e, i, m**), ECV map (**b, f, j, n**), ECG (**c, g, k, o**), and TTE (**d, h, l, p**). **a-d**: A patient with BAV-ASR. **e-h**: A patient with BAV-AS. **i-l**: A patient with BAV-AR. **m-p**: A patient with BAV-no_AS/AR.

Fig. 3 Correlations between QRS voltage parameters by ECG and LVEDVi (**a, b, c, d**) or LVMi (**e, f, g, h**).

Fig. 4 Correlations between e' and LVSVi (**a**) and LVM/EDV (**b**).

Fig. 5 Correlations between ECV and LVMi in each subgroup.

Fig. 6 ROC analysis for the prediction of severe AS (**a**) and severe AR (**b**) by LVMi, prediction of AS_LVH by Sokolow-Lyon product (**c**) and Cornell product (**d**), and prediction of AR_LVH by Sokolow-Lyon product (**e**) and Cornell product (**f**)

Figure 1

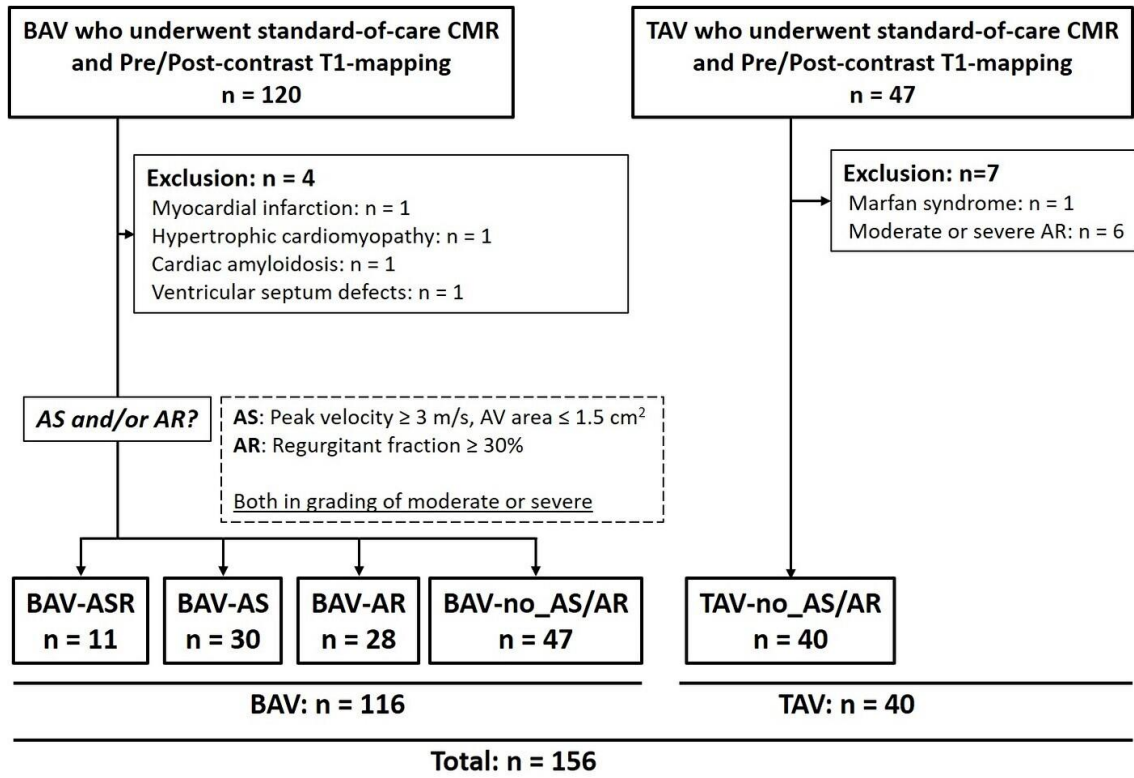


Figure 2

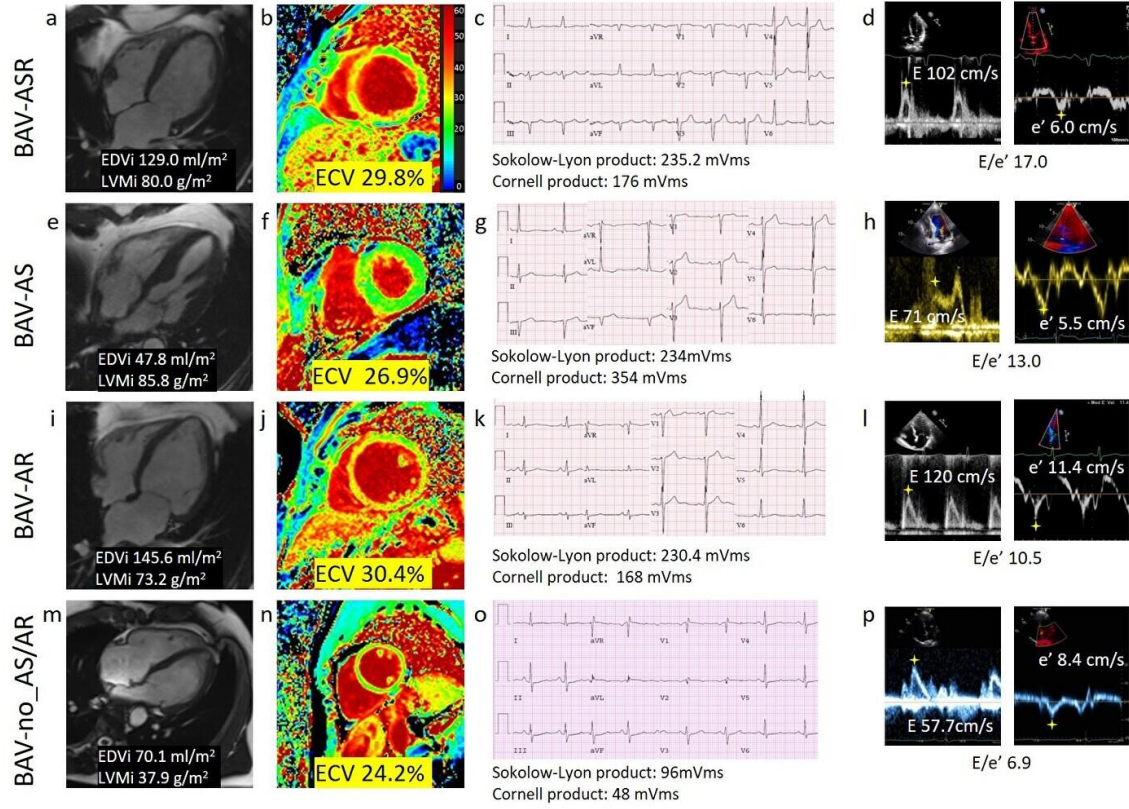


Figure 3

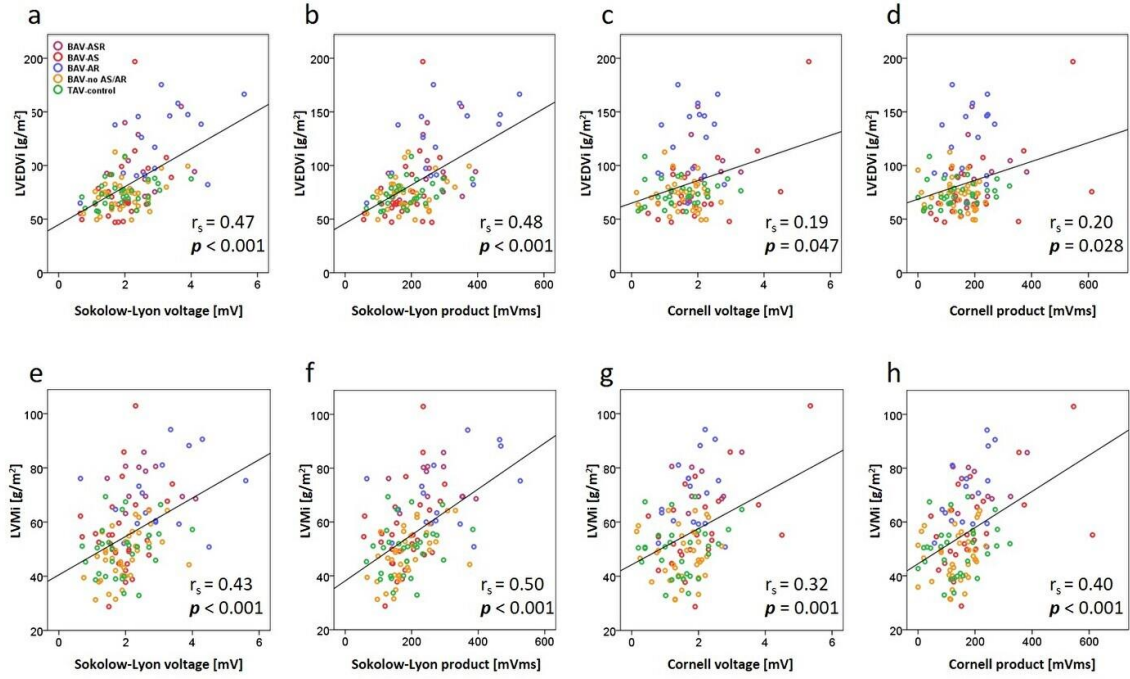


Figure 4

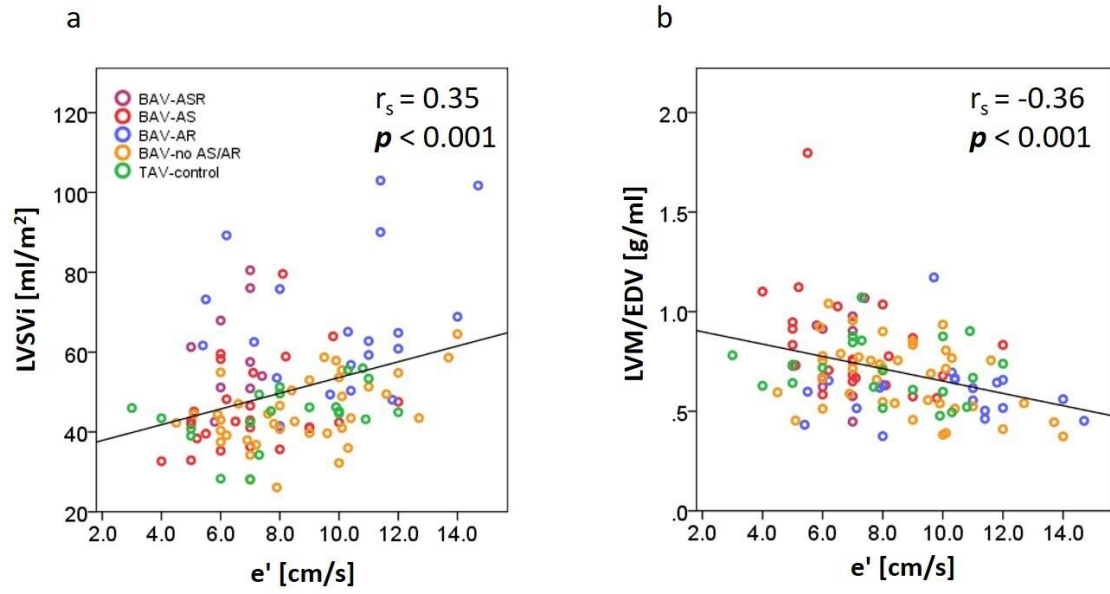


Figure 5

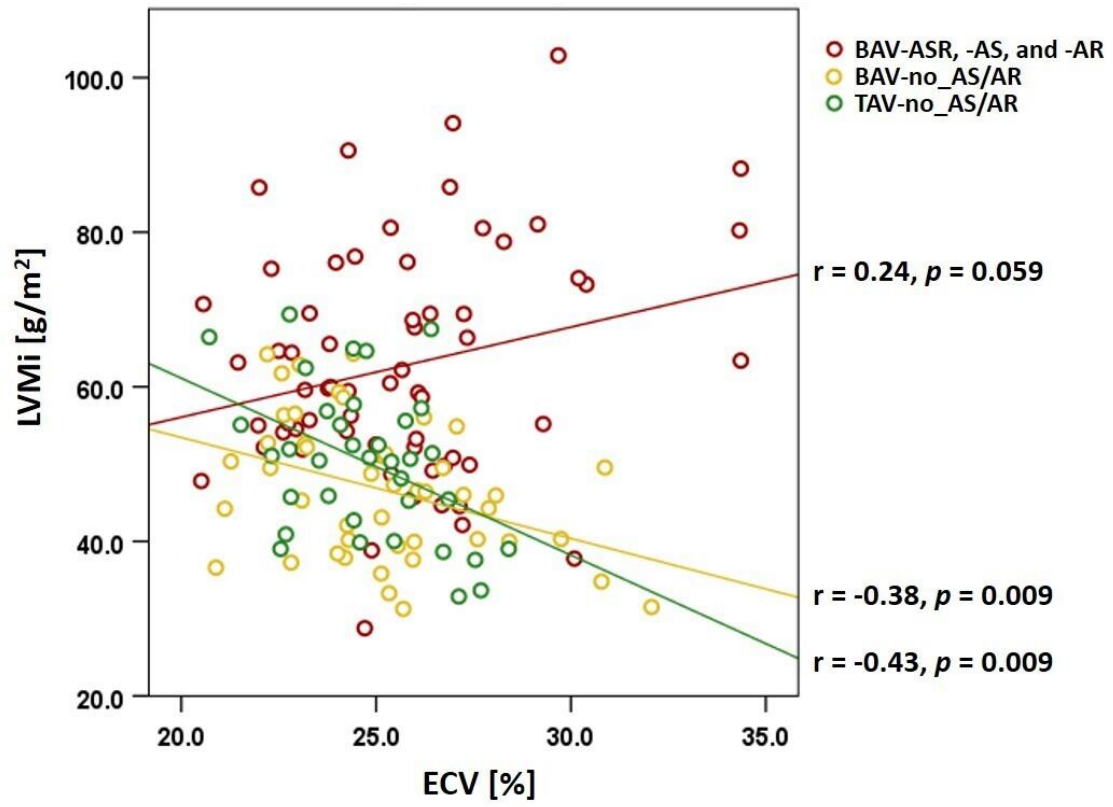


Figure 6

